

4.2 平成 23 年（2011 年）東北地方太平洋沖地震の地震動

本項の論文は、SSA（アメリカ地震学会）のオープンアクセス指針に従った上で掲載している。

(Iwakiri, K. and M. Hoshiya, 2012: High-frequency (>10 Hz) content of the initial fifty seconds of waveforms from the 2011 off the Pacific coast of Tohoku Earthquake, *Bull. Seism. Soc. Am.*, **102**, 2232-2238, doi:10.1785/0120110241)

Bulletin of the Seismological Society of America

This copy is for distribution only by
the authors of the article and their institutions
in accordance with the Open Access Policy of the
Seismological Society of America.

For more information see the publications section
of the SSA website at www.seismosoc.org



THE SEISMOLOGICAL SOCIETY OF AMERICA
400 Evelyn Ave., Suite 201
Albany, CA 94706-1375
(510) 525-5474; FAX (510) 525-7204
www.seismosoc.org

Short Note

High-Frequency (>10 Hz) Content of the Initial Fifty Seconds of Waveforms from the 2011 Off the Pacific Coast of Tohoku Earthquake

by Kazuhiro Iwakiri and Mitsuyuki Hoshihara

Abstract We investigate the high-frequency content of the initial 50 s of waveforms from the 2011 Off the Pacific Coast of Tohoku earthquake (M_w 9.0, 11 March 2011). The strong-motion spectra for the M_w 9.0 mainshock are richer in high-frequency (>10 Hz) content than those of the M_w 7.3 foreshock compared to low frequencies. The mainshock spectra are flat up to at least 20 Hz, which is at variance with the general source spectra models such as the ω -square and f_{\max} models. The spectral ratios of the M_w 9.0–7.3 events show that after 20 s from the P -wave arrival time, the high-frequency strong motion of the mainshock is distributed in the southern Tohoku district. Analyses of past moderate magnitude earthquakes (M_w 6.0–7.3) in the area around the mainshock hypocenter indicate that the radiation from the deeper regions is the main cause of the high-frequency strong motion.

Introduction

The great 2011 Off the Pacific Coast of Tohoku earthquake with a moment magnitude M_w 9.0 (hereafter the 2011 Tohoku earthquake) occurred on 11 March 2011. This thrust-type earthquake along the Japan Trench triggered a devastating tsunami that resulted in a loss of about 20,000 lives (see [Data and Resources](#) section). An area of large slip (>25 m) offshore near the hypocentral region almost coincides with the area of considerable seafloor uplift that generated the tsunami (Yoshida *et al.*, 2011). The region where the strong ground motion occurred during the mainshock extends over an area of approximately 400 km \times 100 km along the Pacific coast between the Tohoku and Kanto districts (Hoshihara *et al.*, 2011).

Initial studies of the 2011 Tohoku earthquake indicate that the high-frequency seismic waves radiated along the down-dip edge of the aftershock zone (e.g., Wang and Mori, 2011; Koper *et al.*, 2011). These findings are based on the back-projection analysis using the teleseismic data, which are reliable for frequencies of up to about 3 Hz. The radiation sources of 4–8 Hz, which were estimated from the regional strong motion data recorded in Japan, were located on the rim of the area of the large slip (Yoshida *et al.*, 2011).

Hoshihara and Iwakiri (2011) showed that the 2011 Tohoku earthquake also radiated high-frequency waves, particularly above 10 Hz, and the frequency content of the waveforms deviated considerably from the empirical relation of the average frequency and magnitude (τ_c - M relation, Wu and Kanamori, 2005). According to the scaling law

described by the ω -square model (Aki, 1967), large earthquakes are expected to be relatively richer in low-frequency content than small earthquakes; however, the seismic waveforms of the M_w 9.0 Tohoku event included a considerable amount of high-frequency (>10 Hz) energy. The frequency contents of great earthquakes such as the M_w 9.0 event provide important information that helps us to evaluate and test this scaling law. However, frequencies above 10 Hz have not been thoroughly examined.

In this study, we investigate the high-frequency components (10–20 Hz in particular) of the 2011 Tohoku earthquake. Then, we estimate the source of the high-frequency waves of the initial 50 s of the 2011 Tohoku earthquake using strong motion records of the past moderate magnitude earthquakes in the region.

Data Processing

Vertical-component strong motion accelerograms of the KiK-net (surface) and K-NET seismic networks (see [Data and Resources](#) section) were used in this study. For spectral analysis, the offsets of the accelerograms were corrected by subtracting the mean of the waveform portion used for each analysis before applying the Fourier transform. Because the stations are close to the source region, these records are expected to contain the long-term change in acceleration due to the static displacement of the mainshock, or a deviation of the baseline of the accelerograms during an event.

After the accelerograms are Fourier transformed, the focus is laid on the high-frequency portions. Therefore, the above-mentioned potential source of deviation has relatively little effect on the analysis, which is presented in this paper. We calculated the signal and noise spectra using a fast Fourier transform of 10% cosine-tapered waveforms. The noise spectrum calculated for the noise portion just before the P -wave arrival was compared with the signal spectrum to determine the suitability of the signal spectrum data for analysis. If the signal-to-noise spectral ratio (S/N) was lower than 3, we excluded the spectrum from the analysis. We calculated the spectral ratios after smoothing each spectrum with a Parzen window of 0.2 Hz bandwidth. Applying the above criteria, 246 stations of K-NET and KiK-net around Tohoku and Kanto district were used in this analysis. The station locations are shown as triangles and crosses in Figure 1. We focused on the spectra in the frequency range of up to 20 Hz, as the frequency of the anti-alias filter of the seismometers used was around 30 Hz.

High-Frequency Waves above 10 Hz

Figure 2a and b shows the Fourier acceleration spectra of the M_w 9.0 mainshock of the 2011 Tohoku earthquake and its M_w 7.3 foreshock (event B1 shown in Fig. 1), respectively, for five time windows: $[t_p, t_p + 10 \text{ s}]$, $[t_p + 10 \text{ s}, t_p + 20 \text{ s}]$, $[t_p + 20 \text{ s}, t_p + 30 \text{ s}]$, $[t_p + 30 \text{ s}, t_p + 40 \text{ s}]$, and $[t_p + 40 \text{ s}, t_p + 50 \text{ s}]$, where t_p is the P -wave arrival time. Figure 2c shows the ratios of the M_w 9.0 spectra relative to the M_w 7.3 spectra for the five time windows, and Figure 2d shows the ratios of the M_w 9.0 event relative to the average spectrum of the five windows of M_w 7.3, as representative of the event (gray line in Fig. 2b). The Fourier acceleration spectra of the M_w 9.0 mainshock of the 2011 Tohoku earthquake (Fig. 2a) is flat up to the frequency of the anti-alias filter ($\sim 30 \text{ Hz}$) after 10 s from t_p , whereas that of the M_w 7.3 foreshock (event B1) tails off at a lower frequency (Fig. 2b), as suggested by Hoshiba and Iwakiri (2011).

According to the ω -square model (Aki, 1967), large earthquakes are expected to have a much lower frequency content than small earthquakes, as the corner frequencies of large earthquakes are lower than those of small earthquakes. Furthermore, f_{\max} (Hanks, 1982), the frequency at which the high-frequency content of the acceleration spectra abruptly diminishes, is expected to exist at frequencies higher than the corner frequency. Because f_{\max} is also found in waveforms recorded at close distance (hypocentral distance $< 10 \text{ km}$), whole path attenuation is not the main factor in the rapid decay of the spectral amplitude (e.g., Hanks, 1982; Archuleta *et al.*, 1982). The reason of f_{\max} is not well understood (e.g., Tsurugi *et al.*, 2009): f_{\max} might be controlled by subsurface characteristics or influenced by source characteristics. In the M_w 9.0 Tohoku event f_{\max} is not evident in the time windows later than $t_p + 10 \text{ s}$ (Fig. 2a). The spectral ratios (Fig. 2c,d) show that although frequency-

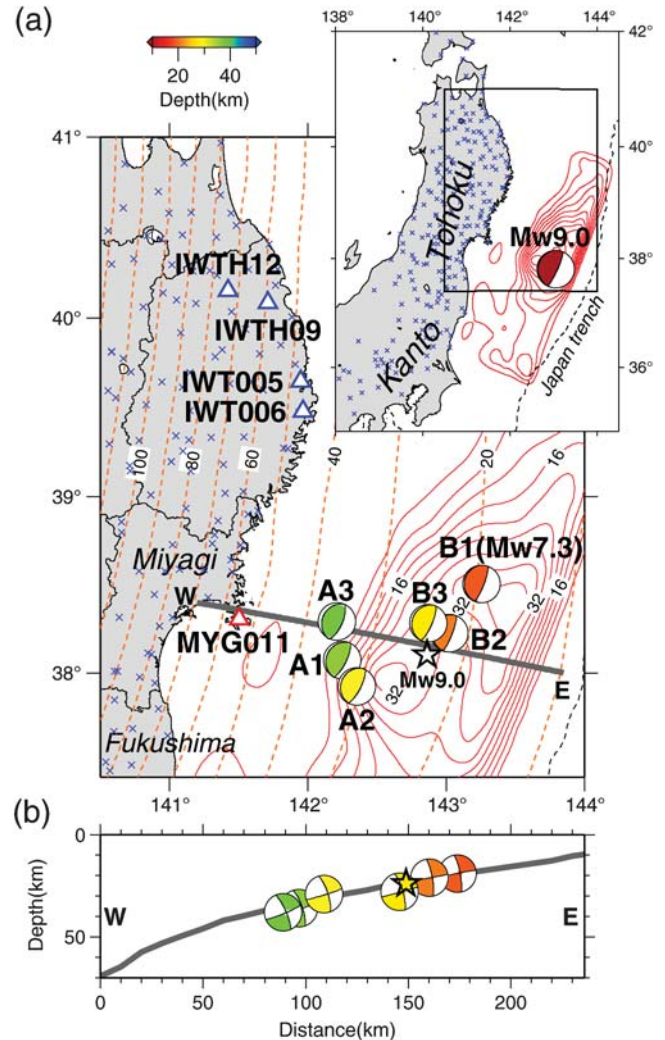


Figure 1. (a) Distribution of earthquakes and seismic stations used in this study. The six earthquakes, labeled A1–A3 and B1–B3, are listed in Table 1 and their centroid moment tensor solutions (determined by the Japan Meteorological Agency [JMA] in the lower hemisphere projection) are shown here. The color scale denotes the centroid depth. Star, the epicenter of the 2011 Tohoku earthquake; crosses and triangles, the 246 seismic stations in KiK-net and K-NET that are used in this study; red contours (contour interval 4 m), the coseismic slip distribution for the 2011 Tohoku earthquake, as estimated from regional strong motion data in the 0.01–0.15 Hz frequency band (Yoshida *et al.*, 2011); and orange broken lines represent the depth of the subducting Pacific slab (Nakajima and Hasegawa, 2006), with 10 km intervals. (b) Cross-section of the subduction zone along the thick gray line in (a).

dependence is not evident for the 10 s time window of $[t_p, t_p + 10 \text{ s}]$, it is clearly present in the later time windows for frequencies above 10 Hz. Thus, after $t_p + 20 \text{ s}$ the M_w 9.0 mainshock contains more high frequencies ($> 10 \text{ Hz}$) than the M_w 7.3 foreshock, which is contrary to the model expectations.

We calculated the spectral ratio of the M_w 9.0 event to the averages of five spectral windows of the M_w 7.3

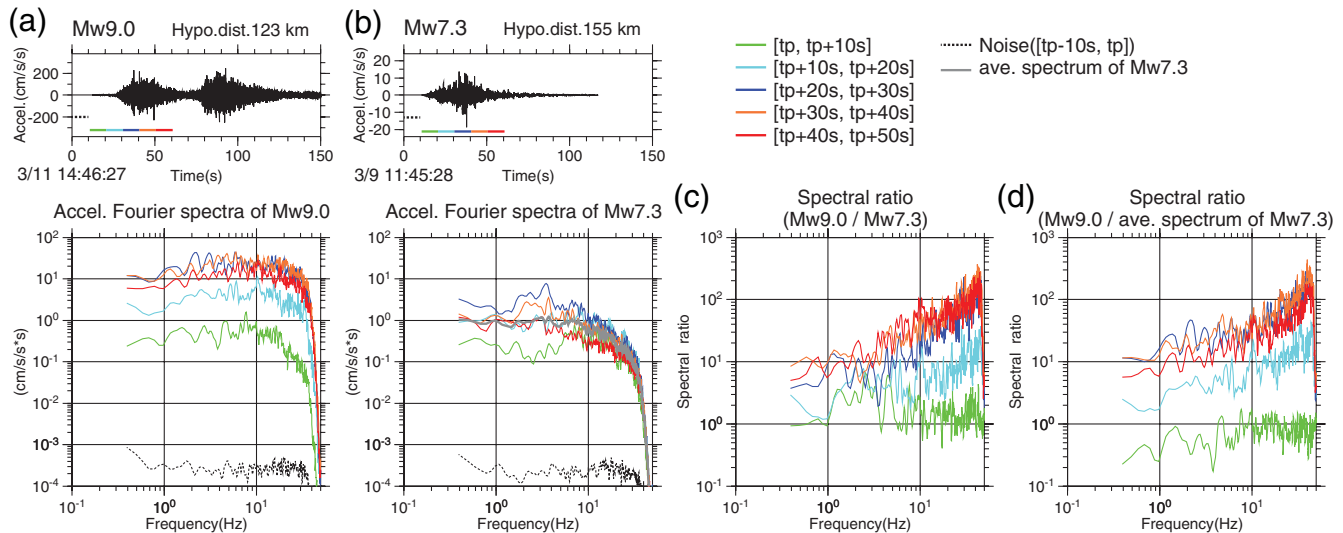


Figure 2. Vertical accelerograms and Fourier spectra from the data recorded at station MYG011 (red triangle in Fig. 1) for (a) the 2011 Tohoku earthquake (M_w 9.0) and (b) its M_w 7.3 foreshock (event B1 of Fig. 1 and Table 1), which is derived from time windows of $[t_p, t_p + 10$ s], $[t_p + 10$ s, $t_p + 20$ s], $[t_p + 20$ s, $t_p + 30$ s], $[t_p + 30$ s, $t_p + 40$ s], and $[t_p + 40$ s, $t_p + 50$ s], where t_p is the P -wave arrival time. Dotted lines indicate noise spectra for the $[t_p - 10$ s, $t_p]$ time window. (c) Spectral ratios of M_w 9.0–7.3 for the five corresponding time windows. (d) Spectral ratios between the five time windows of the M_w 9.0 spectra and the average M_w 7.3 spectrum indicated by the gray line in (b).

foreshock corresponding to five frequency bands for the 246 stations of the KiK-net and K-NET (Fig. 3). For the time windows $[t_p, t_p + 10$ s] and $[t_p + 10$ s, $t_p + 20$ s] (Fig. 3a,b), the spectral ratios are uniformly lower than about 5 across all frequency bands in the Tohoku to northern Kanto district. After $t_p + 20$ s (Fig. 3c–e), the high-frequency spectral ratios are higher than the low-frequency spectral ratios for the stations distributed mainly in the southern part of the Tohoku district. Across the frequency bands 5–20 Hz, the distribution of the high spectral ratios expands mainly in the northwest or west direction from the hypocenter of the M_w 9.0 event.

Source of High-Frequency Waves

To investigate the sources of the high-frequency waves, we analyzed six moderate magnitude (M_w 6.0–7.3) events (Fig. 1; Table 1) that occurred in the region of the 2011 Tohoku earthquake. The six events are divided into two groups (groups A and B) on the basis of their focal depths; group A earthquakes are deeper than the focal depth of the 2011 Tohoku earthquake, whereas group B earthquakes are equal to or shallower than the 2011 Tohoku earthquake. Group A events consist of the Miyagi-Oki earthquake of 2005 and its two aftershocks, and group B events consist of the three foreshocks of the 2011 Tohoku earthquake. All six events are thrust-type earthquakes, as is the 2011 Tohoku earthquake, and they have almost the same focal mechanism (Fig. 1).

We calculated the spectral ratios for pairs of group A and B events of similar magnitude, that is, the spectral ratios of

events A1 to B1, A2 to B2, and A3 to B3 (Fig. 4). The four seismic stations used for these calculations were selected on the basis of the following criteria: (1) all six events of groups A and B were recorded, (2) the distances to the recording station for the two events used to calculate spectral ratios are similar to minimize the difference of path effects, and (3) the S/N is good. S/N for all events except B2 were greater than about 3 for all frequencies; for event B2, S/N was poor, below about 1 Hz, because the signal was contaminated by the coda waves of a previous small earthquake. The spectral ratios for the three event pairs show that the high-frequency content between about 1 Hz and at least 20 Hz is higher in group A events at all stations. In contrast, group B events have a higher content of frequencies below about 1 Hz, although the spectral ratios at low frequencies are less clear than those at high frequencies. This result suggests that the seismic waves radiated from the deeper regions (corresponding to the region of group A) cause high-frequency strong motion more efficiently.

Discussion

Our result, which is derived from Figure 3, shows that after $t_p + 20$ s the distribution of the high-frequency strong motion from the 2011 Tohoku earthquake relative to the M_w 7.3 foreshock expands in the southern Tohoku district. The source of the high-frequency radiation can also be seen in the results of the previous studies. Wang and Mori (2011) concluded that the high-frequency rupture (>1 Hz; reliable up to about 3 Hz) moved northwestward from the hypocenter, and Yoshida *et al.* (2011) indicated that the source of

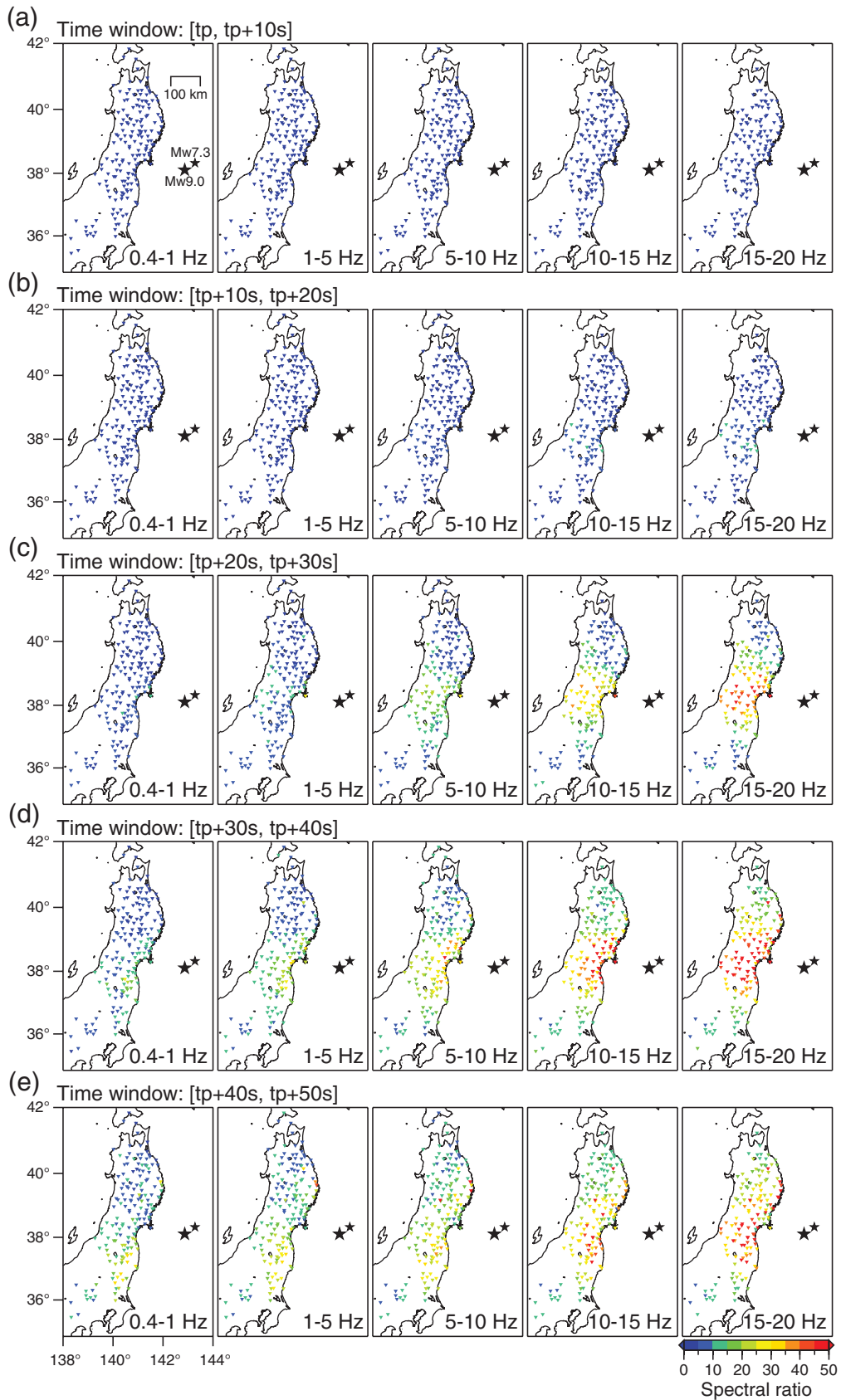


Figure 3. Averages of spectral ratios of the 2011 Tohoku earthquake (M_w 9.0) to its foreshock (M_w 7.3; event B1) for five frequency bands. Fourier spectra of the vertical acceleration of the M_w 9.0 event are derived from five time windows. The spectrum of the foreshock is the average of those obtained from the five time windows.

Table 1
Parameters of the Earthquakes

Event ID	Origin Time* † (yyyy/mm/dd h:m)	Focal Depth* (km)	Centroid Depth* ‡ (km)	M_w * ‡
Group A				
A1	2005/08/16 11:46	42	36	7.1
A2	2005/12/02 22:13	40	29	6.5
A3	2005/12/17 03:32	40	38	6.0
Group B				
B1	2011/03/09 11:45	8	19	7.3
B2	2011/03/10 06:23	9	21	6.4
B3	2011/03/10 03:16	29	28	6.0

*JMA seismic catalog (see [Data and Resources](#) section).

†JST, Japan Standard Time.

‡From centroid moment tensor solutions.

high-frequency radiation (4–8 Hz) was at the western rim of the area of the large slip. These locations are in agreement with the concept that seismic waves radiated from deeper events (in the group A region) cause the high-frequency spectral content, as shown in Figure 4. This regional variation of observed frequency is consistent with the evidence obtained from the rupture of the 2011 Tohoku earthquake (e.g., [Ide et al., 2011](#); [Koper et al., 2011](#); [Lay et al., 2012](#)). Figure 1 shows that the high-frequency events (group A) are located on the edge of the area of the large slip, whereas the low-frequency events (group B) are located within the area where the slip exceeded 24 m. These results suggest that the observed spectra of previous earthquakes in a particular region are consistent with the source properties of the ruptures of the subsequent larger earthquakes in the region. The regional difference of frequency content might be caused by the regional difference of the source radiation and/or path difference between the sources and the observation stations. The unclear distance dependence of the spectral ratio (IWT006 and IWTH12) in Figure 4 suggests that the spectral difference might be attributed to the difference of attenuation around the source region rather than the whole path, even though the path plays a major role in causing the spectral difference. To determine whether the regional difference in the source radiation or the attenuation difference around the source regions is the main factor in affecting the wave spectra, analysis of the high-resolution attenuation structure might be required for the high-frequency range (>10 Hz).

Figure 4 suggests a correlation between f_{\max} and the locations (or the focal depth) of the earthquake rupture. Such frequency dependence was identified in the rupture area of the Sanriku-Oki earthquake of 1994, which occurred north of the 2011 Tohoku earthquake rupture area ([Sato et al., 1996](#)). The 1994 rupture propagated westward from the initial rupture point near the Japan trench and terminated with high-frequency rupture at the deeper part of the inter-plate boundary. [Takemura et al. \(1989\)](#) found a regional dependence of high-frequency and low-frequency earthquakes while analyzing the moderate magnitude (M_w 4–6) events that occurred

at the subduction zone off Fukushima Prefecture: high-frequency inter-plate earthquakes occurred mainly in the northwestern (deeper) part of the region, whereas low-frequency earthquakes occurred in the southeastern (shallower) part. These previous studies and our results suggest that the deeper and shallower sources of the subduction zone tend to cause high- and low-frequency ground motions at the Tohoku district, respectively, not only for individual moderate size earthquakes but also for subevents of a big earthquake.

Conclusions

Strong high-frequency (>10 Hz) waves were observed in southern Tohoku district in the waveforms from the M_w 9.0 Tohoku Earthquake 20 s after the P -wave arrival. Analyses of past events near the hypocenter of the M_w 9.0 event show that waveforms from deeper events contain more high-frequency energy compared to those from shallower events. This result suggests that the rupture in deeper regions caused high-frequency waves not only in individual moderate size earthquakes but also in the subevents of a big earthquake. We also provided evidence stating that f_{\max} of the M_w 9.0 event was higher than expected, and the timing and frequency content suggest that the strong high-frequency (>10 Hz) wave might be associated with the location (or depth) of the earthquake rupture.

Data and Resources

The situation of damage of the 2011 Tohoku earthquake can be found on the Fire and Disaster Management Agency Web page at <http://www.fdma.go.jp/bn/higaihou.html> (last accessed April 2012).

The hypocentral parameters (origin time, location, magnitude, and focal mechanism) for this study, which were routinely determined by the JMA ([JMA, 2011](#)), were retrieved from the JMA seismic catalog ([JMA, 2011](#)) and the JMA Web page at <http://www.seisvol.kishou.go.jp/eq/mech/cmt/top.html> (last accessed April 2012).

Strong motion accelerograms of KiK-net and K-NET ([Okada et al., 2004](#)) were obtained from the National Institute for Earth Science and Disaster Prevention (NIED) at <http://www.kyoshin.bosai.go.jp> (last accessed June 2011).

Acknowledgments

We would like to thank the two anonymous reviewers and the editor Zhigang Peng for their comments that were useful in revising the manuscript. Data from KiK-net and K-NET of National Research Institute for Earth Science and Disaster Prevention (NIED) were used in this analysis. Hypocenter location and focal mechanism of events mentioned in this paper are obtained from the integrated hypocentral catalog of the Japan Meteorological Agency (JMA). All figures were made using Generic Mapping Tools, version 4.2.0 ([Wessel and Smith, 1998](#)).

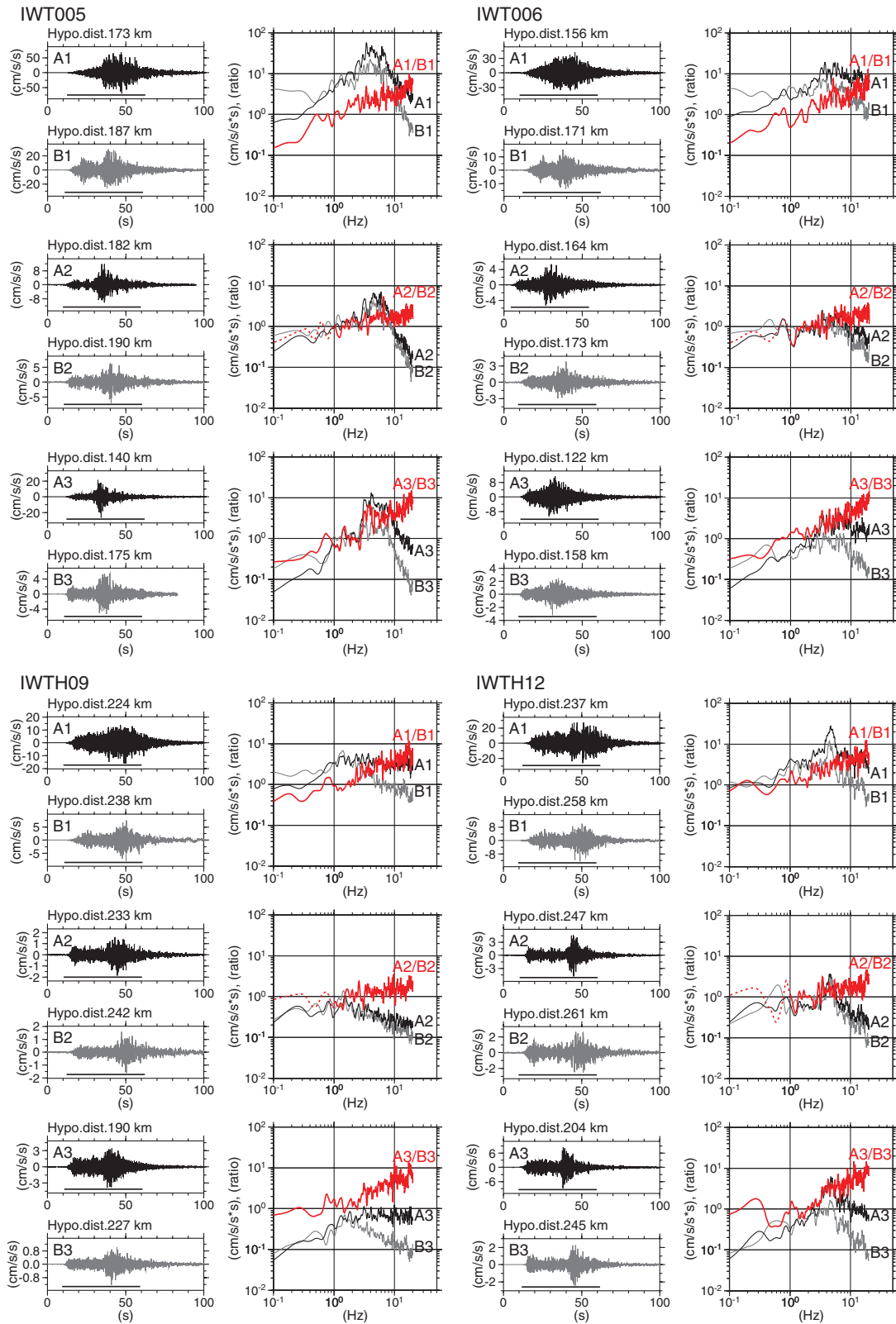


Figure 4. Vertical accelerograms and Fourier spectra of data recorded at stations IWT005, IWT006, IWTH09, and IWTH12 for group A and B events, and spectral ratios of group A to group B for pairs of events of approximately the same magnitude. Details of group A and B events are provided in Figure 1 and Table 1. Seismic station locations are shown in Figure 1. Red lines, the spectral ratios of group A (black) to B (gray); red broken lines, spectral ratios for frequencies lower than about 1 Hz indicate low S/N; and solid lines under the waveforms, time windows $[t_p, t_p + 50 \text{ s}]$ for which are calculated spectra. Hypocentral distance is shown at the top of each waveform.

References

- Aki, K. (1967). Scaling law of seismic spectrum, *J. Geophys. Res.* **72**, no. 4, 1217–1231.
- Archuleta, R. J., E. Cranswick, C. Mueller, and P. Spudich (1982). Source parameters of the 1980 Mammoth Lakes, California, earthquake sequence, *J. Geophys. Res.* **87**, no. B6, 4595–4607.
- Hanks, T. C. (1982). f_{\max} , *Bull. Seismol. Soc. Am.* **72**, no. 6A, 1867–1879.
- Hoshiya, M., and K. Iwakiri (2011). Initial 30 seconds of the 2011 Off the Pacific Coast of Tohoku earthquake (M_w 9.0)—Amplitude and τ_c for magnitude estimation for earthquake early warning, *Earth Planets Space* **63**, no. 7, 553–557.
- Hoshiya, M., K. Iwakiri, N. Hayashimoto, T. Shimoyama, K. Hirano, Y. Yamada, Y. Ishigaki, and H. Kikuta (2011). Outline of the 2011 Off the Pacific Coast of Tohoku earthquake (M_w 9.0)—Earthquake early warning and observed seismic intensity, *Earth Planets Space* **63**, no. 7, 547–551.
- Ide, S., A. Baltay, and G. C. Beroza (2011). Shallow dynamic overshoot and energetic deep rupture in the 2011 M_w 9.0 Tohoku-Oki earthquake, *Science* **332**, no. 6036, 1426–1429.
- Japan Meteorological Agency (JMA) (2011). *The Seismological and Volcanological Bulletin of Japan for January 2011* (CD-ROM), JMA, Tokyo.
- Koper, K. D., A. R. Hutko, T. Lay, C. J. Ammon, and H. Kanamori (2011). Frequency-dependent rupture process of the 2011 M_w 9.0 Tohoku earthquake: Comparison of short-period P wave backprojection images and broadband seismic rupture models, *Earth Planets Space* **63**, no. 7, 599–602.
- Lay, T., H. Kanamori, C. J. Ammon, K. D. Koper, A. R. Hutko, L. Ye, H. Yue, and T. M. Rushing (2012). Depth-varying rupture properties of subduction zone megathrust faults, *J. Geophys. Res.* **117**, no. B04311, 21 pp., <http://www.agu.org/pubs/crossref/2012/2011JB009133.shtml>.
- Nakajima, J., and A. Hasegawa (2006). Anomalous low-velocity zone and linear alignment of seismicity along it in the subducted Pacific slab beneath Kanto, Japan: Reactivation of subducted fracture zone? *Geophys. Res. Lett.* **33**, L16309.
- Okada, Y., K. Kasahara, S. Hori, K. Obara, S. Sekiguchi, H. Fujiwara, and A. Yamamoto (2004). Recent progress of seismic observation networks in Japan—Hi-net, F-net, K-NET and KiK-net, *Earth Planets Space* **56**, xv–xxviii.
- Sato, T., K. Imanishi, and M. Kosuga (1996). Three-stage rupture process of the 28 December 1994 Sanriku—Oki Earthquake, *Geophys. Res. Lett.* **23**, no. 1, 33–36.
- Takemura, M., S. Hiehata, T. Ikeura, and T. Uetake (1989). Regional variation of source properties for middle earthquakes in a subduction region, *Zisin* **2** **42**, no. 3, 349–359 (in Japanese with English abstract).
- Tsurugi, M., T. Kagawa, and K. Irikura (2009). Study on a high-cut filter for strong ground motion prediction (Part 2)—Based on the observed records during the 2005 Fukuoka-ken Seiho-oki earthquake, *J. Japan Assoc. Earthq. Eng.* **9**, no. 1, 1–18 (in Japanese with English abstract).
- Wang, D., and J. Mori (2011). Rupture process of the 2011 Off the Pacific Coast of Tohoku earthquake (M_w 9.0) as imaged with back-projection of teleseismic P -waves, *Earth Planets Space* **63**, no. 7, 603–607.
- Wessel, P., and W. H. F. Smith (1998). New, improved version of Generic Mapping Tools released, *Eos Trans. AGU* **79**, no. 47, 579.
- Wu, Y. M., and H. Kanamori (2005). Experiment on an onsite early warning method for the Taiwan Early Warning System, *Bull. Seismol. Soc. Am.* **95**, no. 1, 347–353.
- Yoshida, Y., H. Ueno, D. Muto, and S. Aoki (2011). Source process of the 2011 Off the Pacific Coast of Tohoku earthquake with the combination of teleseismic and strong motion data, *Earth Planets Space* **63**, no. 7, 565–569.

Seismology and Volcanology Research Department
 Meteorological Research Institute
 Nagamine 1-1
 Tsukuba 305-0031
 Japan
 kiwakiri@mri-jma.go.jp
 mhoshiya@mri-jma.go.jp

Manuscript received 29 August 2011